Theoretical and Applied Climatology
https://doi.org/10.1007/s00704-023-04686-9

RESEARCH

Climate change may cause oasification or desertification both: an analysis based on the spatio-temporal change in aridity across India

Subhra Sekhar Maity[1] · Rohit Prasad Shaw[1] · Rajib Maity[1]

Received: 27 February 2023 / Accepted: 24 September 2023

Abstract
Climate change-induced aridity changes are observed globally and in India, with variable spatial and temporal distribution. Unlike droughts, aridity denotes a persistent climate condition requiring in-depth analysis utilising long-term data to identify any significant spatio-temporal shifts. Given the absence of a comprehensive assessment covering the entire Indian subcontinent, the primary objective of this study is to investigate the spatial change in aridity, its temporal trend, and the change point of its mean values across Indian mainland considering a time period of 1902–2021. Furthermore, this study also investigates the spatio-temporal variations in desertification vulnerability across the Indian mainland. Findings from the study reveal the potential for both desertification and oasification across India's diverse climate regions. Analysis over a period of 120 years (1902 to 2021), the aridity index (AI), which is calculated as a ratio of precipitation (P) and potential evapotranspiration (PET), reveals that eastern and northeast states (20% of total area) show a significant decreasing trend in the aridity index (i.e., increased aridity). In contrast, parts of north-western and southern peninsular India (21% of the total area) show a significant increasing trend (i.e., decreased aridity). This pattern shows a tendency to shift towards dryer condition in the eastern and northeast regions of India, while oasification propensity is seen in the north-western and southern regions. Wherever these changes were observed, 59% of the area experienced a sudden change in mean AI (change point at 5% significance level) between 1950 and 1980, which can be attributed to the shift in the global climate regime during the 1970s and 1980s. Furthermore, spatial extent of sub-humid regions has increased by 6.3% between pre-change point (1902–1951) and post-change point (1982–2021) time period, while semi-arid zones have been found to shrink with time. The change can be mainly attributed to changes in P and PET across India. Overall, this study emphasizes on the potential oasification and desertification trends and the vulnerability towards desertification across India. The findings enhance the understanding of impending desertification/oasification, aiding future agricultural and hydrological planning.

1 Introduction

Aridity is a climatic phenomenon that is primarily identified by a deficiency in the availability of water. As Agnew and Anderson (1992) described, aridity primarily depends on a region's average climatic conditions, generally indicating a lack of moisture. The arid and semi-arid regions, commonly referred to as drylands, are highly vulnerable to desertification (Mirzabaev et al. 2022). Drylands accommodate nearly 40% of the global population (Mirzabaev et al. 2022), and according to observed data, the drylands expanded by about 4–8% during the twentieth century globally and now spanned across roughly 40% of the land area (Feng and Fu 2013; Schlaepfer et al. 2017). In India, the semi-arid region accounts for 42.9% of the gross cropped area, supporting approximately 37% of the total population (Squires and Gaur 2020). The vulnerability of dryland ecosystems to desertification is greatly amplified by the synergistic impacts of anthropogenic climate change, increasing pressures on already limited resources, and the implementation of unsustainable management strategies (El-Beltagy and Madkour 2012).

In contrast to the desertification process, which degrades the productivity of a large area of land along with water, flora, and livestock, oasification improves

✉ Rajib Maity
rajib@civil.iitkgp.ac.in; rajibmaity@gmail.com

[1] Department of Civil Engineering, Indian Institute of Technology Kharagpur, Kharagpur 721302, West Bengal, India

Published online: 16 October 2023

soil moisture, water availability and creates habitats for humans and wildlife (Xue et al. 2019). Anthropogenic activities, coupled with global warming, have amplified the processes of desertification and oasification, resulting in considerable modifications to the dynamics of the atmosphere-water-soil–plant system, particularly in arid and semi-arid areas (Xue et al. 2019). Previous studies have shown evidence of changing patterns of precipitation, temperature, and soil moisture across the globe, including India (Dash and Maity 2021; Dutta and Maity 2022). Globally, extensive aridification across continents can be primarily attributed to the significant rise in greenhouse gas (GHG) emissions and the subsequent increase in temperatures over multiple decades (Bonfils et al. 2020). D'Odorico et al. (2013) showed that a combination of rising aridity and widespread land use practices can cause severe land degradation, which in turn aggravates the effects of climatic change occurring close to the surface and accelerates the process of desertification over time. However, it is worth noting that many arid ecosystems have also demonstrated substantial greening and increased vegetation productivity since the 1980s (Lian et al. 2021) due to climate change (Zhu et al. 2023).

Several studies have also been conducted to analyse the change in aridity across the Indian mainland. Based on data from 1951 to 2005, Ramarao et al. (2019) showed that a reduction in precipitation and a rise in PET have led to an increase in aridity across the bulk of India's semi-arid region. Goparaju and Ahmad (2019) assessed the seasonal aridity across India based on the cropping season and concluded that some districts with sufficient precipitation are experiencing high aridity during the rabi and zaid seasons, which hinders crop production. A study by Sahu et al., (2021) revealed that the dryness and wetness are increasing in different parts of the country. Kalyan et al. (2021) studied the desertification vulnerability index over Bana River basin, a semi-arid region of Rajasthan, and found that the desertification vulnerability has decreased for 30% of the area, whereas it increased for 70% of the area. Such changes can be attributed to the changes (positive or negative) in precipitation and temperature across Rajasthan (Pradhan et al. 2019). Choudhary et al. (2023) demonstrated a consistently decreasing humid condition across northeast India by employing the (Barrow 1992) AI index for the period 1969–2017.

To this end, it is essential to investigate the change in aridity across distinct climatic zones of the Indian mainland by determining the aridity change point over a sufficiently long time period and identifying zones with desertification or oasification trends, thereby facilitating water resource planning and management in various sectors. Before proceeding further, it is worthwhile to note the fundamental difference between aridity and drought, with the former being a long-term climatic condition and the latter being a transient phenomenon based on water deficit.

Aridity is defined based on various indices in several studies. Budyko's aridity index is used by Oguntunde et al. (2006) to examine the trends in aridity across the Volta River Basin in West Africa. The worldwide aridity phenomena have been studied by Huang et al. (2016) and (Asadi Zarch et al. 2015) using the United Nations Environment Programme (Barrow 1992) and United Nations Educational, Scientific and Cultural Organization (UNESCO 1979) aridity indices, respectively. De Martonne, (1926) aridity index is used in a study by Zhang et al. (2009) to examine the underlying trends in aridity across the Pearl River basin in South China, whereas Huo et al. (2013) utilised the Thornthwaite (1948) aridity index to detect the trends in aridity over northwest China. Sahu et al. (2021) and Goparaju and Ahmad (2019) have considered Thornthwaite and Mather (1955) aridity index and UNESCO (1979) aridity index respectively, to examine the aridity across India. Among the indices used, those based on precipitation along with potential evapotranspiration (PET) are accepted widely because of their robustness owing to the inclusion of critical meteorological variables like temperature, solar radiation, atmospheric humidity, wind, surface albedo (Yang and Yang 2012). For instance, the emerald city of Seattle, Washington receives, on average, 950 mm of precipitation each year. However, the climate of Dallas, Texas, which likewise receives 950 mm of precipitation annually on average, appears significantly dryer (Scheff and Frierson 2015). This is because of the higher temperatures and dry air, which help to evaporate more water from plants and soil. Therefore, when quantifying climatic aridity, P relative to PET must be considered (Hartmann 1994).

While the findings of the aforementioned studies pertaining to aridity offer valuable insights, they are constrained by their utilization of a limited time span, which may not be enough to capture the long-term shift in aridity and may not accurately represent the long-term trend in aridity across India's diverse climate. In addition, the aforementioned studies have not attempted to identify the change point at which such shifts in aridity occurred, which may be an essential component in comprehending why it occurs. Hence, a comprehensive analysis of the aridity index as well as desertification vulnerability utilising long-term data is essential for the assessment of potential desertification and oasification tendencies, if any, as it is evident that there is a spatial redistribution of rainfall patterns across many parts of the world as well as India (Maity and Maity 2022; Schlef et al. 2023). Thus, the aim of this study is to investigate

the possible desertification/oasification trend, along with identification of such change points and assessment of spatio-temporal changes in desertification vulnerability index (DVI) across the Indian mainland between 1902 and 2021 on a decadal and annual scale. Furthermore, the study also tries to quantify any changes in the spatial extents of aridity-based climate zones. For this purpose, internationally recognized UNESCO (1979) aridity index is utilised because the usage of a single aridity index enables a quantitative evaluation of the spatial pattern and builds a better conceptualization of the underlying trends in aridity. However, the present study only explores the changes in aridity during the observed period which could potentially shift in a positive or negative direction in the future.

2 Study area

As stated, the entire Indian mainland constitutes the study area (Fig. 1). India has a total land area of 3,287,263 km^2 that encompasses multiple climatic zones between latitudes 8.4°N and 37.6°N and longitudes 68.7°E and 97.25°E. The Indian Ocean bounds India to the south, the Arabian Sea to the southwest, and the Bay of Bengal to the east. The administrative division of India consists of 28 states and 8 union territories. Roughly 60% of the total land area is used for agricultural purposes, while nearly 22% is forest land (Ahmad et al. 2019). Southwest monsoon during June–September contributes about 80% of total annual rainfall over India (Sahu et al. 2021). India exhibits diverse bioclimatic variations, and the ongoing climate change is expected to influence it (Shukla et al. 2017).

3 Data and methodology

3.1 Data used

The current study uses the monthly mean precipitation (P) and potential evapotranspiration (PET) data to compute the aridity index. The data for the aforementioned variables are collected from the Climatic Research Unit (CRU) (https://crudata.uea.ac.uk/cru/data/hrg/ accessed on October 2022), which is continuously being improved and maintained by principally UK's Natural Environment Research Council (NERC) and the United States Department of Energy for the entire globe. These datasets relate to the Climatic Research Unit (CRU)

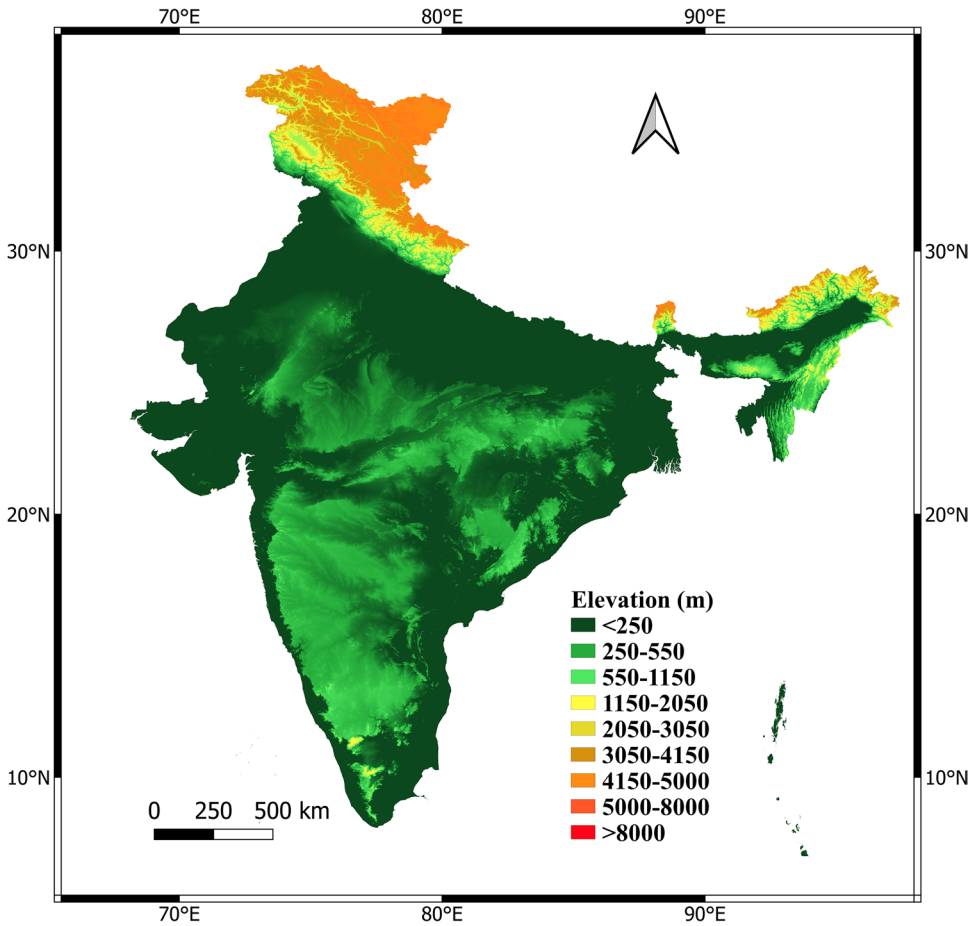

Fig. 1 Digital Elevation Model (DEM) of the study area (Indian mainland) generated from Shuttle Radar Topography Mission (SRTM) data (https://www.earthdata.nasa.gov/)

gridded time Series version 4.06 (CRU TS v. 4.06) (Harris et al. 2020). For this analysis, precipitation and PET data from CRU TS v. 4.06 datasets are obtained for the period of 1902 to 2021 with 0.5˚×0.5˚ (55 km×55 km) horizontal grid resolution across the Indian mainland. The CRU datasets are based on in situ observations and have proven to perform well in different regions across the globe (Sun et al. 2018; Shen et al. 2021). Various quality-control techniques, including the exclusion of outliers and short records, have been employed in the compilation of the most recent CRU database (Harris et al. 2020). Recent hydro-climatological research conducted around the globe has utilised CRU data with great effectiveness (Ahmed et al. 2020).

Penman–Monteith equation is used to calculate the PET data in the CRU database (Harris et al. 2020) as it offers the best estimate of PET compared to other formulas and also suggested by the Food and Agriculture Organization (FAO) (Koutroulis 2019). The Penman–Monteith equation has been adopted in several studies to calculate PET (Lickley and Solomon 2018; Salam et al. 2020). Additionally, for DVI, the digital elevation model (DEM) is obtained from the Shuttle Radar Topography Mission (SRTM) (https://www.earthdata.nasa.gov/ accessed on August 2023). Soil texture data is obtained from Regridded Harmonized World Soil Database v1.2 (https://daac.ornl.gov/cgi-bin/dsviewer.pl?ds_id=1247 accessed on August 2023) (Wieder 2014) and soil depth data is obtained from the National Remote Sensing Centre (NRCS) archive of Bhuvan (https://bhuvan-app3.nrsc.gov.in/data/download/index.php accessed on August 2023). Further description of the dataset to calculate DVI is described in Section 3.4.

3.2 Aridity indices

Aridity indices can quantify the degree of water scarcity in a given region due to long-term climate change. Typically, aridity is measured as a function of annual mean precipitation. For instance, a typical precipitation-based definition of an arid region is one with fewer than 250 mm of precipitation per year. The Intergovernmental Panel on Climate Change (IPCC) utilised this criterion for aridity (IPCC 2007). Semi-arid locations are often characterised by yearly precipitation between and (250 and 500 mm). Aridity indexes that have achieved general recognition consider all three criteria, whether directly or indirectly. Although there is consensus regarding the broad location of arid regions, there is disagreement regarding the methods used to distinguish the specific boundaries of territories with varying degrees of aridity (Agnew & Anderson 1992). Several other aridity indices have also been introduced, primarily based on potential evapotranspiration (PET). Some of these indices are (1) Thornthwaite aridity index (Thornthwaite 1948), (2) Erinc's aridity index (Erinç 1965), (3) United Nations Environment Programme (Barrow 1992) aridity index, and (4) United Nations Educational, Scientific and Cultural Organization (UNESCO 1979) aridity index.

In this study, we have used the aridity index (AI) formulated by UNESCO 1979, which is based on the ratio of annual precipitation and potential evapotranspiration and expressed by Eq. (1) as follows:

$$\mathrm{AI} = \frac{P}{PET} \tag{1}$$

where, PET is calculated using the Penman–Monteith formula (Penman 1948; Monteith 1965; Zotarelli et al. 2014). Thus, the index is conceptually simple and requires only precipitation and potential evapotranspiration data. However, the index bears a signature of different hydrometeorological characteristics, such as temperature, relative humidity, precipitation, solar radiation, and wind speed. Based on this index, five aridity classes are defined, and the details are provided in Table 1.

3.3 Statistical analysis

In this study, non-parametric statistical tests like Sen's Slope estimator (Sen 1968) combined with modified Mann–Kendall (m–MK) test (Hamed and Ramachandra Rao 1998) is used to determine the decadal trend, rate of change of AI as well as the corresponding area at 0.05 significant level. Pettitt test (Pettitt 1979) is used to determine the change point in the mean aridity index at an annual scale. Non-parametric tests like Pettitt test and m-MK test methods are less sensitive to outliers and missing values in a time series (Ullah et al. 2019); hence, it is robust and resilient compared to parametric ones (Wang 2006). Furthermore, it does not require prior distribution knowledge or data normality and is less sensitive to unexpected gaps in a time series (Conover 2006).

The Mann–Kendall (MK) test is an effective method for detecting trends in a time series. However, the presence of positive autocorrelation increases the likelihood of identifying a trend even when one does not exist (Hamed and Ramachandra Rao 1998). The m-MK test is an improvement over the MK test, as it includes an autocorrelation correction

Table 1 Classification of aridity index (AI) based on UNESCO (1979) (Asadi Zarch et al. 2015)

Classifications	Aridity index (AI)
Hyper arid	AI < 0.03
Arid	0.03 < AI < 0.2
Semi-arid	0.2 < AI < 0.5
Sub humid	0.5 < AI < 0.75
Humid	AI > 0.75

coefficient (Eq. (5)) to remove errors caused by autocorrelation in a time series, if present.

In addition, the Innovative Polygon Trend Analysis (IPTA) (Şen et al. 2019) is also employed to compare the results obtained from the m-MK test. IPTA is unaffected by autocorrelation and is mathematically simple (Şen et al. 2019). However, in the present study, results from the m-MK test are utilised for further analysis, while IPTA is used only to verify the trend pattern obtained from the m-MK test.

Pettitt test is frequently employed for change point detection as it is not restricted by distributional assumptions and is effective in identifying a single dominant change point (Shukla et al. 2023; Soorya Gayathri et al. 2023). In the subsequent section, the m-MK test and Pettitt test are explained briefly. The detailed methodology for IPTA can be found in Şen et al. (2019).

3.3.1 Modified Mann–Kendall test (m-MK)

The most frequent method for detecting trends in hydrometeorological time series data is the modified Mann–Kendall (m–MK) test, which is a non-parametric, two-tailed statistical test based on rank system (Hamid and Ramachandra Rao, 1998). As a first step, data are detrended, and then the effective sample size is determined by ranking the coefficients of significant serial correlation. The null hypothesis (H_o) of the m-MK test states that there is no monotonic trend in the intended significance level against the alternative hypothesis (H_a) that the data follow a monotonic trend. The test statistics is given by Eq. (2) as follows:

$$S = \sum_{i=1}^{n-1} \sum_{j=i+1}^{n} \operatorname{sign}\left(x_j - x_i\right) \tag{2}$$

where n indicates the total number of data, and x_j and x_i denote the data points of time i and j. $\operatorname{sign}\left(x_j - x_i\right)$ is given by Eq. (3).

$$\operatorname{Sign}\left(x_j - x_i\right) = \begin{Bmatrix} = +1 \text{ if } x_j - x_i > 0 \\ = 0 \text{ if } x_j - x_i = 0 \\ = -1 \text{ if } x_j - x_i < 0 \end{Bmatrix} \tag{3}$$

The variance of S, modified VAR(S), can be estimated using Eq. (4) as (Hamed and Ramachandra Rao 1998):

$$\operatorname{VAR}(S) = \frac{1}{18}\{n(n-1)(2n+5)\}\left(\frac{n}{n_e^*}\right) \tag{4}$$

The autocorrelation correction coefficient $\left(\frac{n}{n_e^*}\right)$ is evaluated by Eq. (5) as follows:

$$\left(\frac{n}{n_e^*}\right) = 1 + \frac{2}{n(n-1)(n-2)} \sum_{i=1}^{n-1} (n-i)(n-i-1)(n-i-2)\rho(i)_s \tag{5}$$

In this equation, $\rho(i)_s$ represents the autocorrelation across ranks of calculated observations, and n is the optimal number of observations for calculating autocorrelation in data.

The standardized test measurement Z is given by Eq. (6) as follows for $n > 10$:

$$Z = \begin{cases} \frac{S-1}{\sqrt{\operatorname{VAR}(S)}}, & \text{if } S > 0 \\ 0, & \text{if } S = 0 \\ \frac{S+1}{\sqrt{\operatorname{VAR}(S)}}, & \text{if } S < 0 \end{cases} \tag{6}$$

At a significance level of $\alpha = 0.05$, a Z-score greater than 1.96 (Z critical) indicates a significant positive trend, whereas a Z-score less than -1.96 indicates a significant negative trend, and the trend is insignificant when the value falls within -1.96 and + 1.96.

3.3.2 Pettitt test

Detecting the change points is one of the most crucial components of analysing climatic and hydrological data series (Gao et al. 2011). The non-parametric method, devised by Pettitt (1979), permits the identification of a significant change point in a time series when the exact timing of the change is uncertain. The null hypothesis states that there is no change point in the series; the alternative hypothesis is that there is a change point, which is characterised by two samples, such as $x_1, x_2 \ldots, x_m$ and $x_{m+1}, x_2 \ldots, x_n$ are from the same population. The test statistic $U_{t,n}$ is given by Eq. (7):

$$U_{t,n} = \sum_{i=2}^{n} \cdot \sum_{j=1}^{i-1} sign(X_i - X_j) \tag{7}$$

where sign is defined by Eq. (8):

$$\operatorname{Sign}\left(X_i - X_j\right) = \begin{Bmatrix} +1 if\left(X_i - X_j\right) > 0 \\ 0 if\left(X_i - X_j\right) = 0 \\ -1 if\left(X_i - X_j\right) < 0 \end{Bmatrix} \tag{8}$$

The test statistic calculates the instances in which a member of the first sample is greater than a member of the second sample. Most of the unique change points are identified at the point where the magnitude of the test statistics |Ut, n| is maximum.

Pettitt Test Statistic for two tail tests is given by Eq. (9):

$$K_T = Max|U_{t,n}|, 1 \le t < n \tag{9}$$

When $|U_{t,n}|$ is maximum, the associated confidence level (p) for the sample length (n) may be described by Eq. (10) as:

$$p = 2exp\left(\frac{-6{K_T}^2}{n^3 + n^2}\right) \quad (10)$$

Once the p-value falls below the predetermined significance level of 0.05, the null hypothesis can be rejected, and the data can be divided into two subseries (before and after the transition point).

3.4 Desertification Vulnerability Index (DVI)

In the present study, the areas sensitive to desertification are identified by calculating the desertification vulnerability index (DVI) (Kalyan et al. 2021). DVI is generally calculated as the geometric mean of several other indices such as climate quality index (CQI), soil quality index (SQI), socioeconomic quality index (SoQI) and so on (Xu et al. 2019; Kalyan et al. 2021; Perović et al. 2021). In this study, we have utilised only CQI and SQI to calculate DVI (Eq. (11)). Further the changes in DVI between the pre-change point (1902–1951) and the post-change point (1982–2021) (refer to Section 4.4) are analysed to identify the regions with increased or decreased DVI. The equation of DVI is given by Eq. (11) as follows:

$$DVI = (CQI \times SQI)^{1/2} \quad (11)$$

The indices and necessary additional data to calculate DVI are described in the subsequent sections.

3.4.1 Climate Quality Index (CQI)

The Climate Quality Index (CQI) relates the impact of climate variation with desertification sensitivity. In this study, it was estimated based on the following three parameters: mean annual precipitation, AI, and slope-aspect. The annual precipitation is obtained from CRU data as described in Section 3.1 and AI is calculated as per Section 3.2. Slope aspect is calculated from a digital elevation model obtained from Shuttle Radar Topography Mission (SRTM) (https://www.earthdata.nasa.gov accessed on August 2023) and resampled to the same resolution as CRU using QGIS 3.32.2 software. Subsequently, the values of these three parameters are assigned weights, and the geometric mean values of these weights are calculated to determine the CQI utilising Eq. (12), which is as follows:

$$\text{CQI} = (\text{annual precipitation} \times \text{aridity index} \times \text{slope aspect})^{1/3} \quad (12)$$

The values and assigned weights for the parameters of CQI are listed in Table 2.

3.4.2 Soil Quality Index (SQI)

The Soil Quality Index (SQI) measures the effect of the landscape as well as the soil conditions on desertification. The SQI considers the slope of the terrain, soil texture, and soil depth to quantify the region's resilience against desertification, or, in other words, how vulnerable it is to desertification. Generally, a higher slope is associated with decreased soil stability, which is prone to erosion (Siswanto and Sule 2019). Soil texture and depth also have significant impacts on land desertification. Soils with shallow depth and a high proportion of sand have a reduced water-holding capacity and are more susceptible to erosion (Xu et al. 2019). Due to changing climate, regions with such soil features are generally more sensitive to desertification. The SQI is calculated using Eq. (13) as follows (Siswanto and Sule 2019; Kalyan et al. 2021; Perović et al. 2021):

$$\text{SQI} = (\text{Slope} \times \text{Soil texture} \times \text{Soil depth})^{1/3} \quad (13)$$

The slope is calculated from DEM obtained from Shuttle Radar Topography Mission (SRTM) (https://www.

Table 2 Description of parameters used to obtain the Climate Quality Index (CQI). Low to high values of weights indicate very good to very poor resilience against desertification, respectively

Parameter	Description	Weight	References
Annual precipitation (mm)	> 1000	1	Xu et al. (2019); Perović et al. (2021)
	650–1000	1.33	
	280–650	1.67	
	< 280	2	
Aridity	Humid (> 0.75)	1	Asadi Zarch et al. (2015); Perović et al. (2021)
	Dry sub-humid (0.5–0.75)	1.33	
	Semi-arid (0.2–0.5)	1.67	
	Arid (0.03–0.2)	2	
Slope aspect	Flat	1	Xu et al. (2019)
	West, Northwest, North	1.33	
	Northeast, East	1.67	
	Southeast, South, Southwest	2	

earthdata.nasa.gov accessed on August 2023) and resampled to the same resolution as CRU using QGIS 3.32.2 software. Soil texture data is calculated from Regridded Harmonized World Soil Database v1.2 (https://daac.ornl.gov/cgi-bin/dsviewer.pl?ds_id=1247 accessed on August 2023) (Wieder 2014) and Soil depth data is obtained from the National Remote Sensing Centre (NRCS) archive of Bhuvan (https://bhuvan-app3.nrsc.gov.in/data/download/index.php accessed on August 2023). The description and weights of the parameters are listed in Table 3.

4 Results and discussions

4.1 Spatial distribution of precipitation (P) and potential evapotranspiration (PET)

The spatial distribution of precipitation (P) and potential evapotranspiration (PET) plays a vital role in comprehending the aridity within a particular region. While previous studies have adequately outlined the spatial patterns of P and PET across various time periods (Mukherjee et al. 2015; Lakshmi et al. 2019), it remains necessary to provide an overview of these patterns before looking into an in-depth analysis of aridity trends across India. From 1902 to 2021, mean annual precipitation varied from less than 100 mm to more than 4000 mm across India, with an average of 1093 mm (Fig. 2a). Maximum precipitation is noted across the western ghat region and north-east India, while lower precipitation is observed across the north-western region of the country and the leeward side of the western ghat. Furthermore, the coefficient of variation (CV) of precipitation is observed to be highest in the lowest precipitation regions, such as Gujarat, followed by Rajasthan, while the minimum CV is noted in parts of southern India, such as Kerala, eastern India, and northeast India (Fig. 2b).

The mean annual potential evapotranspiration across India during the period of 1902–2021 varies from less than 700 mm to more than 1900 mm, with a mean of 1451 mm (Fig. 2c).

The highest value of PET is observed across the western part, followed by southern and central India, which can be attributed to high temperatures, strong wind, and dry climate. A gradual decline in PET is observed towards India's northeastern and northern regions. Regions with the lowest mean PET showed the highest CV (Fig. 2d). This pattern is particularly evident in areas such as Ladakh, Jammu and Kashmir (J&K), followed by north-east India. From Fig. 2, it can be observed that zones with lower precipitation approximately coincide with the region with high PET demand. Low-precipitation regions with high PET are potentially more susceptible to aridity change (Ramarao et al. 2019). However, confirming the occurrence of any such changes necessitates additional investigation, as described in the subsequent sections.

Table 3 Description of parameters used to obtain the Soil Quality Index (SQI). Low to high values of weights indicate very good to very poor resilience against desertification, respectively

Parameter	Description	Weight	References
Texture*	L, SCL, SL, LS, CL	1	Kosmas et al. (1999)
	SC, SiL SiCL	1.33	
	Si, C, SiC	1.67	
	S	2	
Slope (%)	< 6	1	Kosmas et al. (1999)
	6–18	1.33	
	18–35	1.67	
	> 35	2	
Soil depth (cm)	> 75	1	Kosmas et al. (1999)
	30–75	1.33	
	15–30	1.67	
	< 15	2	

*L, loamy; *SCL*, sandy clay loam; *SL*, sandy loam; *LS*, loamy sand; *CL*, clayey loam; *SC*, sandly clay; *SiL*, silty loam; *SiCL*, silty clay loam; *Si*, silt; *C*, clay; *SiC*, silty clay, *S*, sand

4.2 Trend analysis

Since aridity is a prolonged climatic condition, understanding its underlying trend necessitates considering longer time scales, such as decades. In this study, the aridity index is calculated considering UNESCO (1979) aridity index, as described in Section 3.2. The m-MK test is used to analyse the nature of the trend in conjunction with Sen's slope estimation to determine the trend's slope at a significance level of 0.05, if any. Results show that the aridity index exhibits a mixed spatial pattern of significant increasing (decreasing aridity) and decreasing trend (increasing aridity) across the country (Fig. 3). Similar trend results are obtained from the IPTA test (Section 3.3), as shown in Fig. S1. Among the regions showing a significant trend, 20% of the area experienced a significant decreasing trend in Aridity index (i.e., increasing dryness), covering Nagaland, Mizoram, Manipur, Tripura, Assam, Meghalaya, Arunachal Pradesh, Jharkhand, East Uttar Pradesh, Chhattisgarh, Bihar, and East Madhya Pradesh). Approximately 23% of the area experienced a significant increasing trend (i.e., decreasing dryness), which includes Telangana, Andhra Pradesh, North Karnataka, Maharashtra, Punjab, North Rajasthan, Ladakh and Jammu & Kashmir.

Interestingly, the areas dominated by monsoon precipitation show increasing dryness, whereas areas predominantly dry

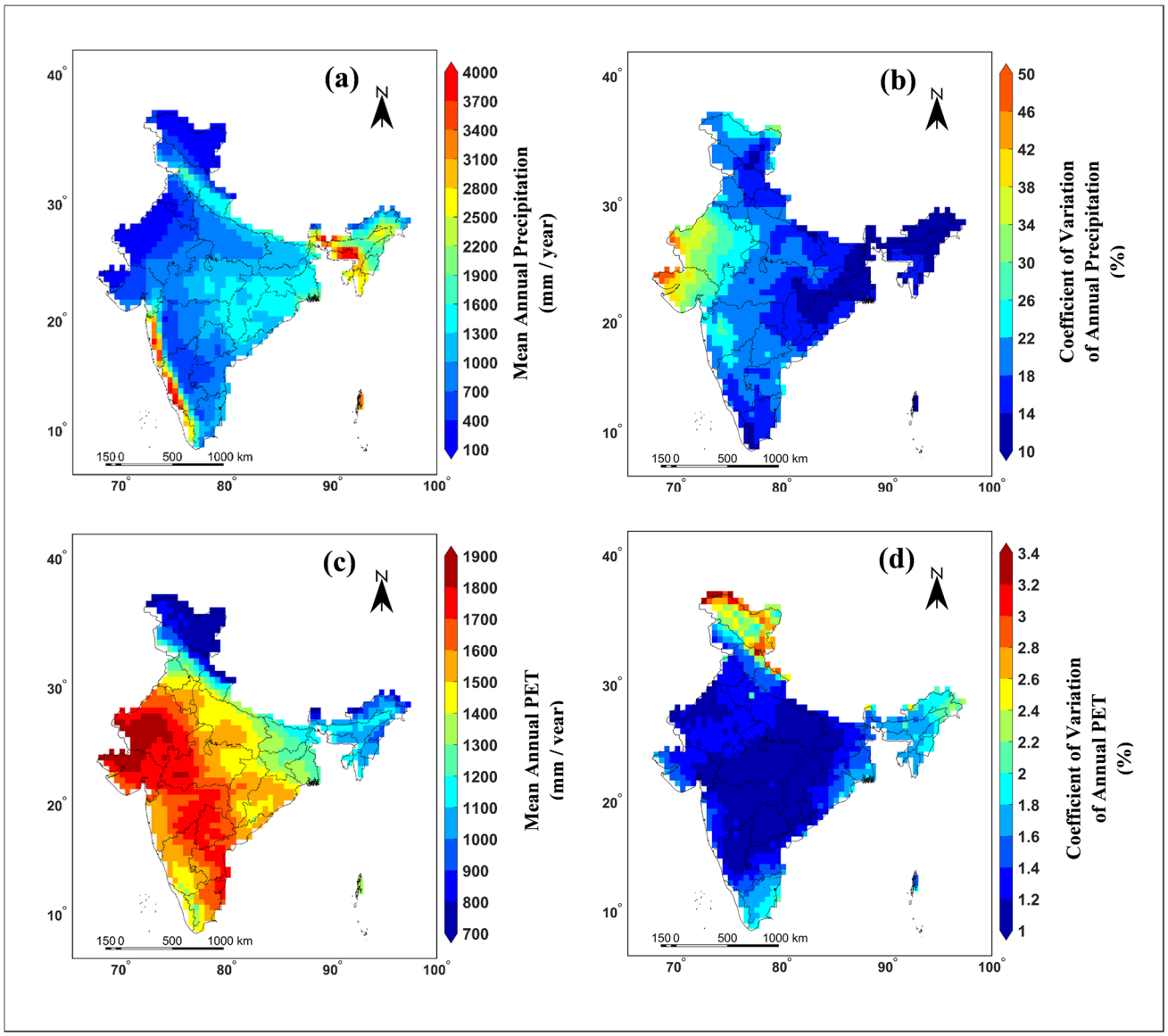

Fig. 2 Maps showing (**a**) mean annual precipitation (mm), (**b**) coefficient of variation (CV) (%) of annual precipitation, (**c**) mean annual potential evapotranspiration (mm), (**d**) coefficient of variation (CV) (%) of annual potential evapotranspiration over the period 1902–2021

show increasing wetness. The variation noticed from the results could be linked with the different climate variables used in this index, i.e., precipitation and PET. Guhathakurta and Rajeevan, (2008) demonstrated that a part of the southern peninsula, the coastal portion of Maharashtra, and the Kashmir region have a trend of significantly increasing annual precipitation, whereas a portion of northern and central India has a trend of significantly decreasing annual precipitation. Conversely, Goroshi et al. (2017) reported that Southern India has a trend of significantly decreasing evapotranspiration, while northern and northeastern India have a trend of significantly increasing evapotranspiration. Mondal et al. (2015) showed that such contrasting precipitation trends can be attributed to climate change, whereas Chattopadhyay and Hulme (1997) showed the same but for PET. It is evident from the results of the aforementioned existing studies that such contrasting trends in aridity obtained in the present study can be directly attributed to climate change. These studies also indicate that precipitation and potential evapotranspiration contribute significantly to the trend in aridity over northern and southern India. In contrast, potential evapotranspiration is the primary contributor in northeast India.

Next, we computed the rate of change in the aridity index using Sen's slope estimator (Sen 1968). Sen's slope is defined as the median of $\left\{\frac{x_j - x_i}{j-i}\right\}$, for $i = 1, 2, 3, 4 \ldots .N$, j > i, where x_j and x_i represent values of time series data at j and i times, and N represents the number of pairs of time series

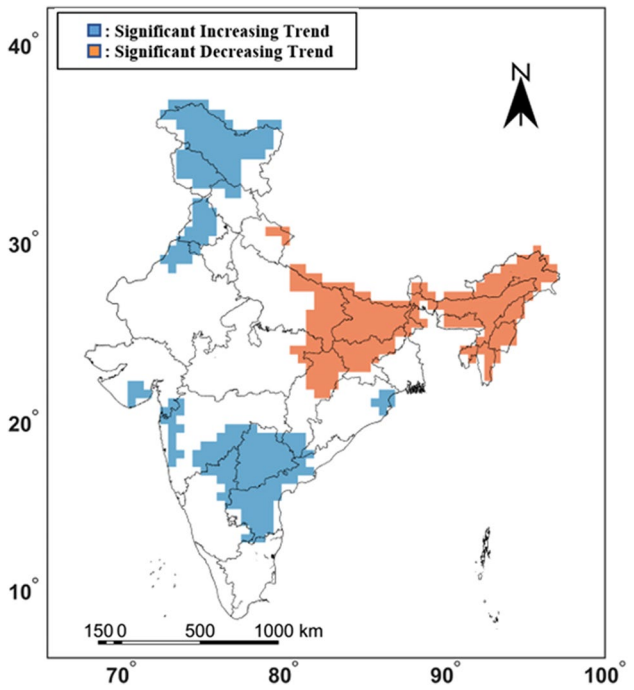

Fig. 3 Modified Mann–Kendall (m-MK) trend analysis of aridity index (AI) at 5% significant level where increasing trend indicates increasing Aridity index (decreasing aridity) and decreasing trend indicates decreasing aridity index (increasing aridity)

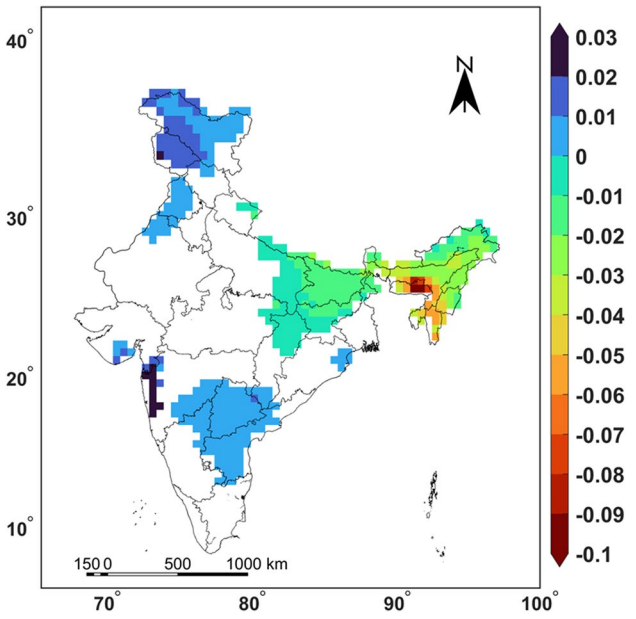

Fig. 4 Spatial map of rate of change in aridity index (per decade) during 1902–2021

elements (x_i,x_j). The spatial map of the aridity index change rate at decadal scale for the period of 1902–2021 is presented in Fig. 4. It is noticed from the results that northeast India has the highest negative change rate of-0.11 /decade, whereas western ghat has the highest positive change rate of 0.035/decade, followed by J&K.

4.3 Variation of the spatial extents of various climatic zones based on aridity

The variations in the yearly extent of hyper-arid, arid, semi-arid, sub-humid, and humid areas (%) during 1902 to 2021 are shown in Fig. 5. Furthermore, it provides insight into the cyclic behaviour of different categories of aridity during the time period. However, the trend in the spatial extent of different aridity-based zones is not reflected on a yearly scale but is visible in a decadal scale (Fig. 6).

Table 4 illustrates the decade wise spatial extent (in percentage of total area of the Indian mainland) of the arid, semi-arid, sub-humid, and humid areas, which varies from 8.09% to 6.73%, 30.85% to 22.57%, and 39.35% to 44.53% respectively from first to last decade of the time period, whereas, the area percentage of the hyper-arid zone is negligible in decadal analysis. The trend results show a significant increasing trend for the sub-humid zone (0.58% per decade), whereas a decreasing trend is observed for the semi-arid zone (-0.41% per decade). The humid zone also indicates a decreasing trend, however, of a small magnitude (-0.19% per decade). On the other hand, the change in the arid zone is negligible. The expansion in sub-humid zones, accompanied by a reduction in semi-arid and humid zones, indicates a potential redistribution of climate aridity that could lead to the oasification and desertification of semi-arid and humid regions, respectively.

4.4 Change point analysis

We utilised the Pettitt test to identify the years with sudden changes in mean AI, as described in Section 3.3.2. Figure 7a shows the spatial map of change points for the aridity index in each grid point over India and the corresponding p-value (Fig. 7b). The results show that most of the significant change points of mean AI across the Indian mainland lie between 1950 and 1980, covering around 59% of the area with a significant increasing/decreasing trend.

Next, we considered two specific points to demonstrate the increasing (Fig. 8) and decreasing (Fig. 9) change points. In Fig. 8, a change point corresponding to the latitude and longitude of 15.25°N, 78.25°E is depicted, which is located in Illurukothapalle, Andhra Pradesh. Here, the change point was observed in 1954, accompanied by a sudden increase in the mean aridity index. Similarly, Fig. 9 illustrates a sudden decrease in the mean aridity index at Baisagopalganj, Bihar (latitude 26.25°N and longitude 87.75°E), where the change point was noted in 1956. The result of the change point analysis is then utilised to divide the study period

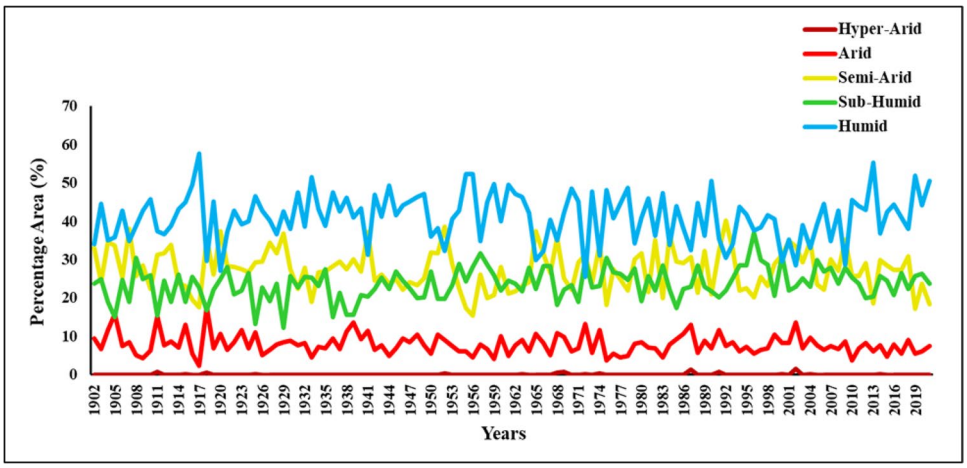

Fig. 5 Percentage area under five different zones based on aridity index on an annual scale for the time period 1902–2021

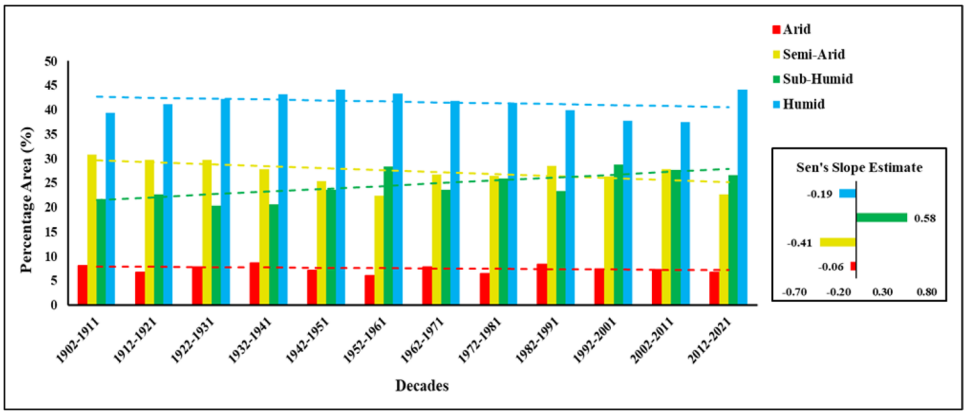

Fig. 6 Percentage area and the corresponding trend and Sen's slope estimate under five different zones based on aridity index on a decadal scale for the period of 1902–2021

Table 4 Decadal variation of the spatial extent of hyper-arid, arid, semi-arid, sub-humid, humid climatic zones during 1902–2021

Decade	Spatial extent of climatic zones (in percentage of entire Indian mainland)				
	Hyper arid	Arid	Semi-arid	Sub humid	Humid
1902–1911	0.00	8.09	30.84	21.72	39.35
1912–1921	0.00	6.64	29.64	22.66	41.06
1922–1931	0.00	7.75	29.73	20.27	42.25
1932–1941	0.00	8.60	27.77	20.53	43.10
1942–1951	0.00	7.07	25.30	23.51	44.12
1952–1961	0.00	6.05	22.40	28.28	43.27
1962–1971	0.00	7.84	26.75	23.60	41.82
1972–1981	0.00	6.39	26.41	25.89	41.31
1982–1991	0.00	8.35	28.45	23.34	39.86
1992–2001	0.00	7.33	26.24	28.79	37.65
2002–2011	0.00	7.24	27.77	27.60	37.39
2012–2021	0.00	6.73	22.57	26.58	44.12

into two time periods, 1902–1951, and 1982–2021, in order to investigate any oasification or desertification tendency across India before and after the occurrence of a sudden change in average aridity, which also coincides the global climate regime shift in the 1970s and 1980s (Reid et al. 2016).

4.5 Oasification/desertification analysis

Comparison of the spatial extent of different climatic zones between the two time periods 1902–1951 and 1982–2021 reveals that the sub-humid region has expanded by 6.3%, whereas arid region, semi-arid region, and humid region have decreased by 0.5%, 3.3%, and 2.5%, respectively. Map showing the areas that are converted to sub-humid regions from semi-arid and humid regions is presented in Fig. 10. The semi-arid regions converted into sub-humid regions are primarily situated in the southern peninsula across Maharashtra, Karnataka, Andhra Pradesh and Telangana, indicating a potential oasification. On the contrary, humid zones converted to sub-humid areas are mainly concentrated over the Gangetic plains covering parts of Uttar Pradesh, Bihar, and Madhya Pradesh. These observations coincide with the trend analysis results described in Section 4.2. In addition, the spatial distribution of aridity pattern over 12 decades is also shown in Fig. 11,

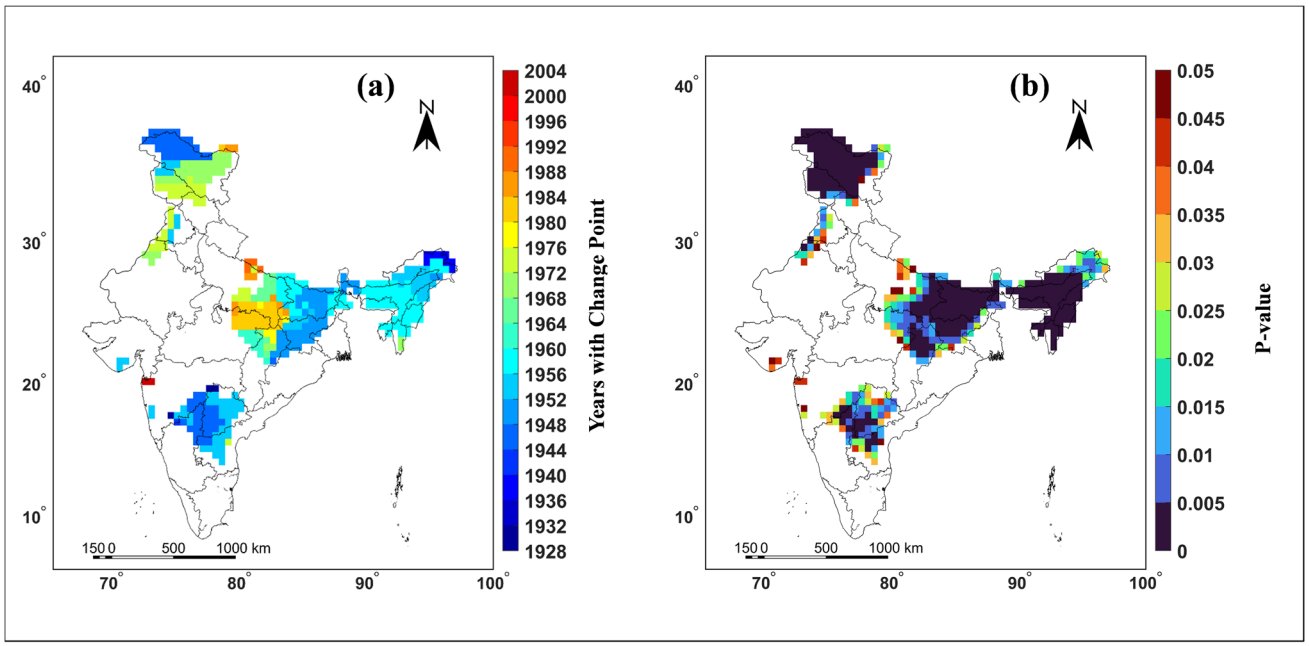

Fig. 7 Spatial maps of (**a**) years with change points in the mean of the aridity index (AI), and (**b**) corresponding probability Value (p-value < 0.05) for the period 1902–2021 at 5% significant level

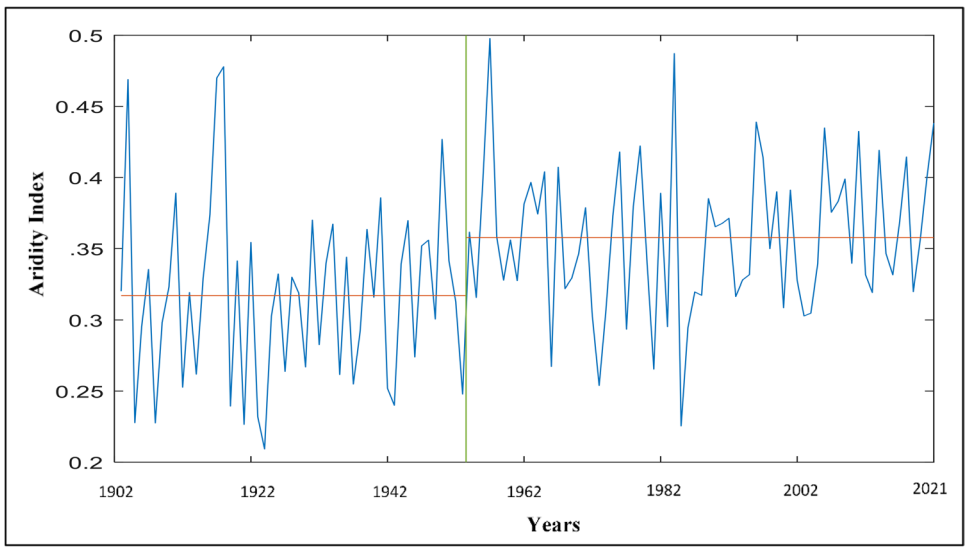

Fig. 8 Plot representing the change in aridity index value over Illurukothapalle, Andhra Pradesh

which shows the gradual increase of sub-humid zones and gradually shrinking semi-arid regions. Although the decrease in semi-arid regions is the primary contributor to the increase in sub-humid regions, the increasing trend of aridity in humid regions may become a major contributor in the future which requires further investigation.

Increasing aridity in some regions of the Gangetic plains indicates a potential vulnerability to the propensity for desertification. Conversely, decreasing aridity in historically semi-arid regions in southern and western India suggests a tendency towards oasification. To better understand the desertification/oasification propensity, the desertification vulnerability index (DVI) is investigated in the subsequent sections.

4.6 Desertification vulnerability Index (DVI)

The Climate Quality Index (CQI), a component used in calculating the Desertification Vulnerability Index (DVI), is depicted in Fig. 12 for both the pre- and post-change point periods. The range of CQI values observed lies between 1 and 2. A higher value indicates greater vulnerability to desertification in relation to factors such as precipitation, aridity, and slope aspect. Conversely, a lower value indicates

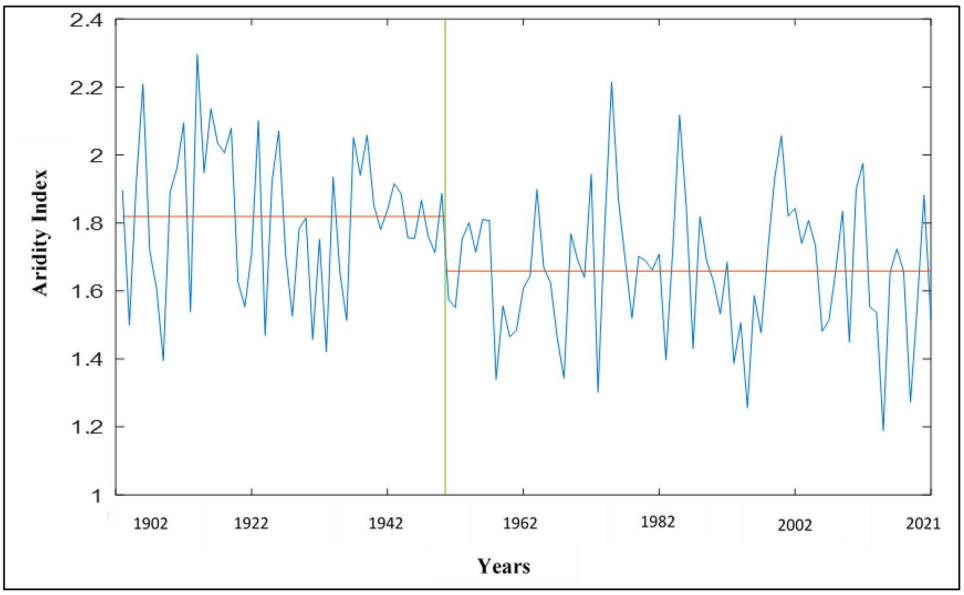

Fig. 9 Plot representing the change in aridity index value over Baisagopalganj, Bihar

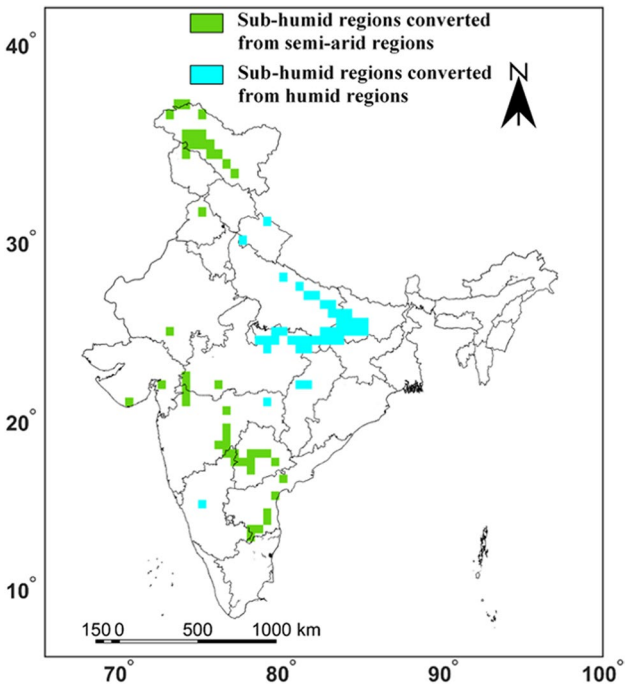

Fig. 10 Regions converted from semi-arid and humid regions to sub-humid regions in 1982–2021 compared to 1902–1951

a lower vulnerability to desertification. The results obtained for the Climate Quality Index (CQI) coincide with the aridity-based zones, demonstrating that humid and sub-humid zones are the least vulnerable to desertification, whereas arid and semi-arid zones are the most vulnerable. However, a shift in the CQI from the pre-change point to the post-change point period can be observed from the figures, which indicate that the CQI has increased in the post-change period for the humid region. In contrast, it has decreased for the semi-arid and sub-humid regions.

Next, we examine the Soil Quality Index (SQI) (Fig. 13). The SQI value ranges from 1 to 1.65, wherein a higher value indicates soils with low resilience, while a lower value indicates a higher resilience to desertification. The results reveal that a significant portion of Eastern India and parts of the Southern, Western, Northwest, and Northeast regions exhibit a favourable SQI. The result also points out that despite having more sandy soil (Fig. S2) than Maharashtra and Madhya Pradesh, Rajasthan has lower weights in SQI. Such characteristics are possible because the soil depth in Maharashtra and Madhya Pradesh is comparatively lesser than in Rajasthan (Fig. S3). The highest vulnerability is observed towards Ladakh and J&K regions.

Next, the DVI is calculated as the geometric mean of CQI and SQI for the pre- and post-change point periods and represented in Fig. 14, along with the changes in DVI between the aforementioned periods. The results indicate a significant increasing shift in the DVI across parts of the Gangetic plains and Madhya Pradesh, along with several other regions scattered throughout India. However, parts of southern, western, and northern India showed a significant decrease in DVI. Comparing Fig. 10 and Fig. 14c, it is evident that the regions converted from humid and semi-arid to sub-humid show increasing and decreasing DVI change, respectively. However, apart from those regions, other areas in southern India (parts of Karnataka, Telangana, Andhra Pradesh, and Maharashtra), western India (part of Gujarat) and northern India (part of Ladakh and J&K) show a decreasing DVI. These changes indicate a propensity towards oasification, which can be mainly attributed to increasing P and decreasing PET (Mondal et al. 2015; Goroshi et al. 2017).

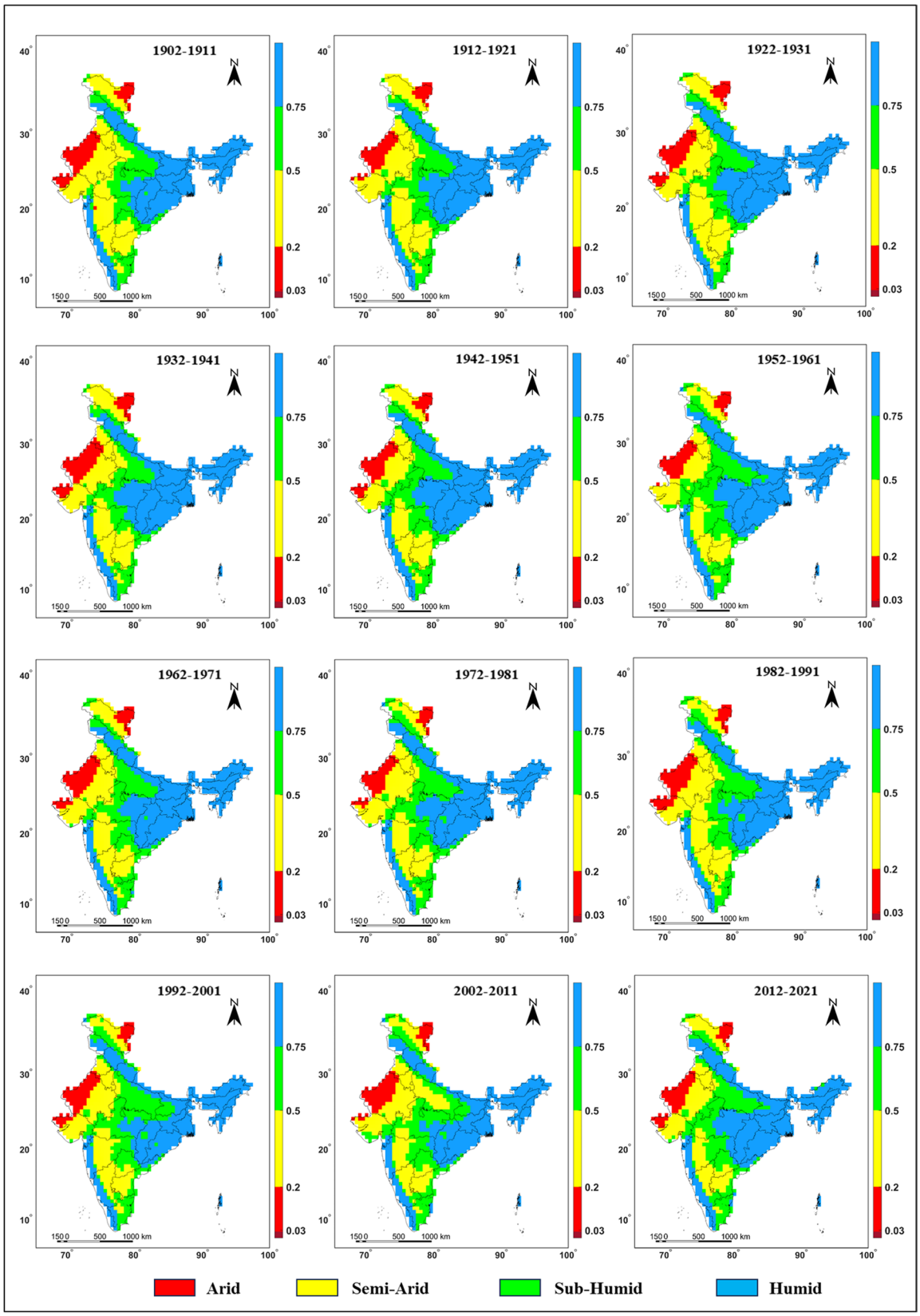

Fig. 11 Map showing changes in aridity over consecutive 12 decades across Indian mainland

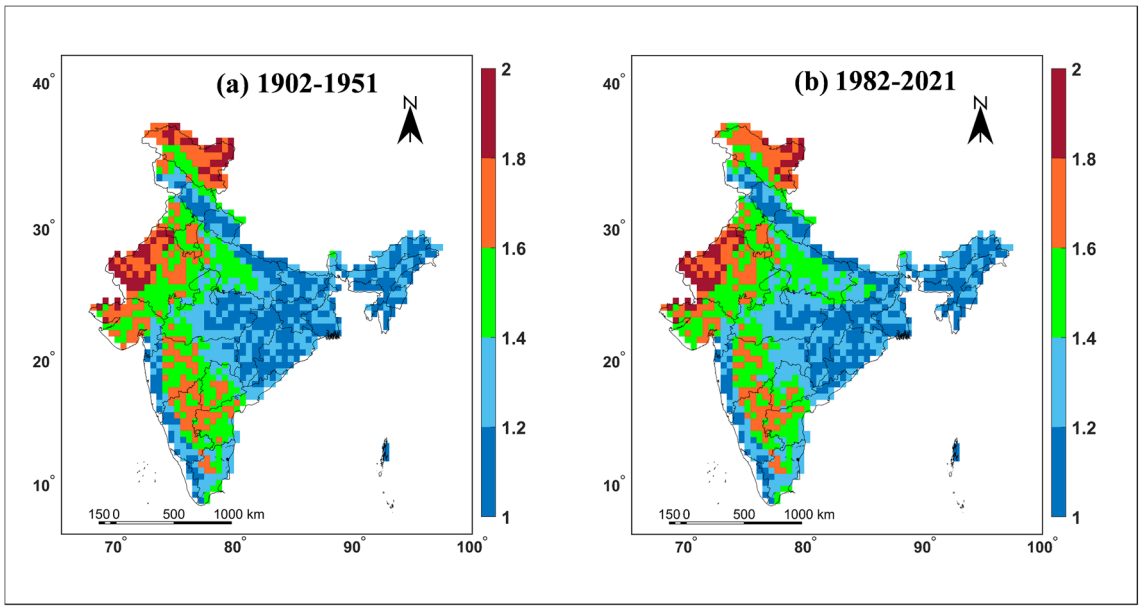

Fig. 12 Climate Quality Index (CQI) map of India where a higher value indicates high vulnerability and a lower value indicates less vulnerability to desertification in terms of annual rainfall, aridity, and slope aspect for the period of **a** pre-change point: 1902–1951 and **b** post-change point: 1982–2021

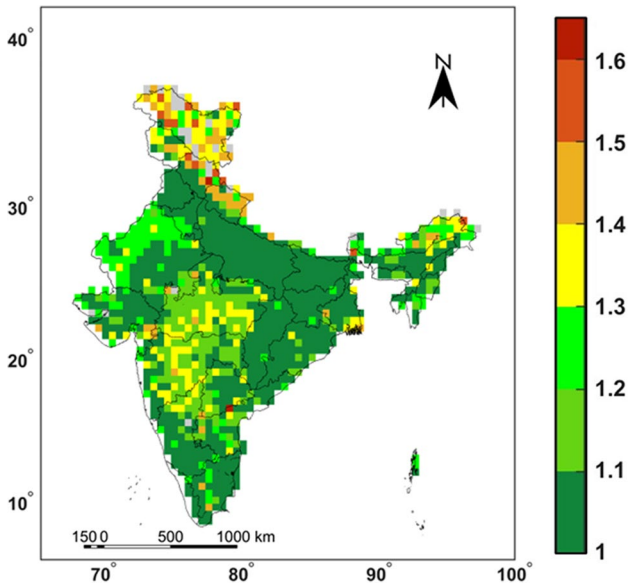

Fig. 13 Soil Quality Index (SQI) map of India, where a higher value indicates high vulnerability and a lower value indicates less vulnerability to desertification regarding soil texture, soil depth, and terrain slope. Grey colour indicates grids with no data

5 Conclusions

The present study explored the detailed spatio-temporal characteristics of aridity across the Indian mainland to evaluate its magnitude and extent. Overall, India's hyper-arid and arid zones cover about 8% of the geographical area, including parts of Rajasthan, Gujarat, Punjab and Haryana and Ladakh. Semi-arid, sub-humid, and humid zones cover about 28%, 24%, and 40%, respectively. The trend analysis revealed decreasing aridity over part of Southern India and J&K and increasing aridity over eastern, northeast, and part of northern India. A sudden change in mean aridity between 1950 and 1980 is captured over 59% of the area, showing a significant trend. The decadal trend analysis revealed that the spatial extent of the sub-humid region is significantly increasing, whereas it is decreasing for the semi-arid region. In accordance with the aforementioned, sub-humid region spans over 27.68% of the total area in the period of 1982–2021 compared to 21.38% during 1902–1951. The 6.3% spatial expansion of sub-humid region is mainly due to the conversion of semi-arid regions in southern and western India, leading to oasification. Although the changes are noticed mainly between semi-arid and sub-humid areas, the increasing dryness over the humid region requires further investigation based on future climate change scenarios. Furthermore, the DVI analysis indicates that the parts of southern, western, and northern India show a significant decrease in DVI compared to the parts of the Gangetic plains, which show a significant increase. These changes mostly coincide with the changes in aridity before and after the change point period. These findings indicate a tendency towards oasification over the southern peninsula, western, and northern India. The decrease in aridity and the increased vulnerability to desertification in the Gangetic plains may be partially attributed to the region's heightened

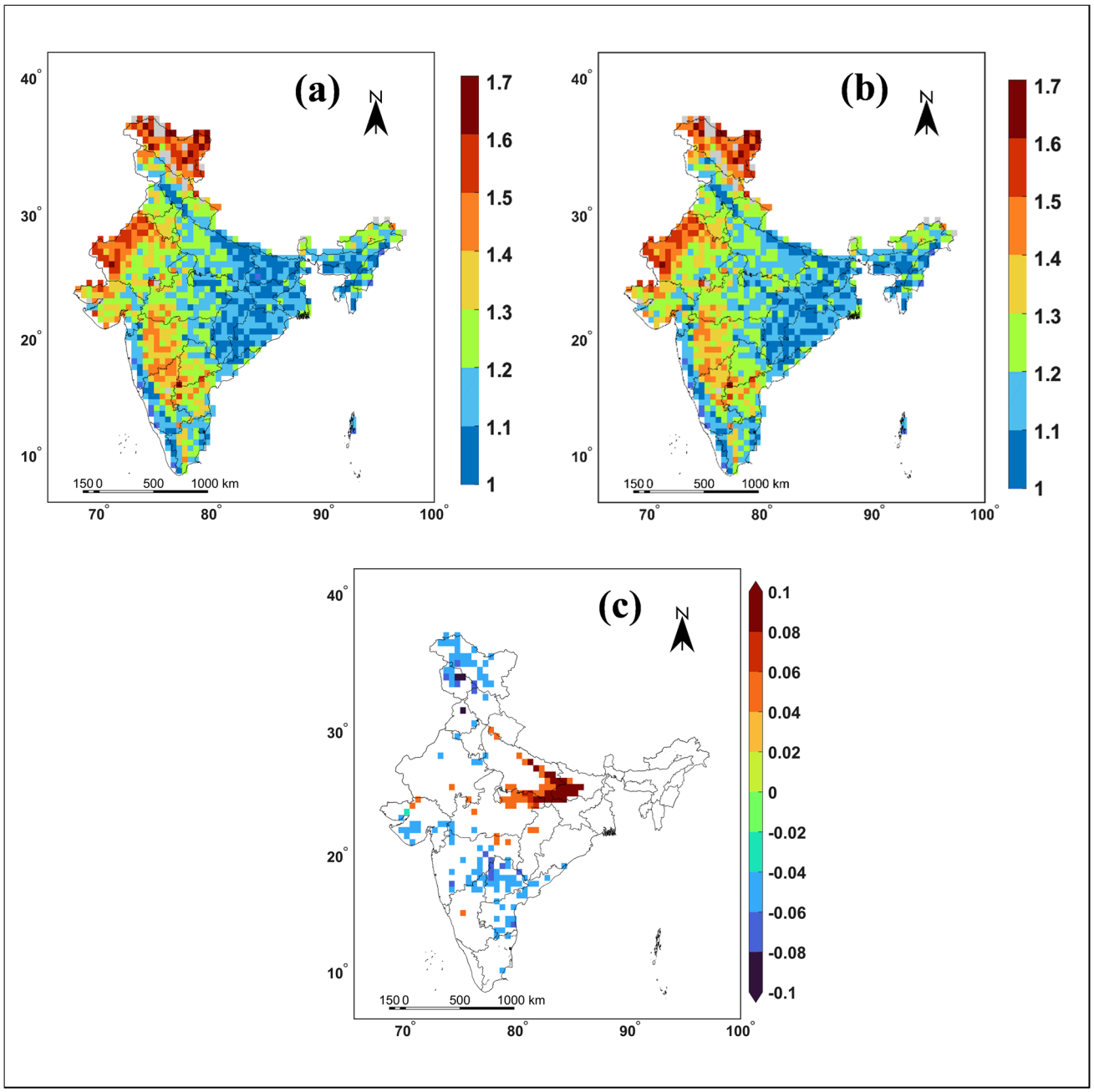

Fig. 14 Desertification Vulnerability Index (DVI) map of India where a higher value indicates high vulnerability and a lower value indicates less vulnerability to desertification in terms of combined SQI and CQI. The DVI is shown for (**a**) pre-change point: 1902–1951 and (**b**) post-change point: 1982–2021. The changes in DVI between pre- and post-change are represented in (**c**)

groundwater extraction for irrigation (Dangar and Mishra 2021). That, in turn, raises the potential evapotranspiration (PET), and when combined with decreasing precipitation, it adversely affects the level of aridity. Whereas, in parts of South and North India, decreased aridity can be primarily attributed to increased precipitation and decreased potential evapotranspiration due to climate change (Chattopadhyay and Hulme 1997; Mondal et al. 2015).

Overall, the findings from this study reveal both positive and negative aspects of climate change on aridity. Oasification in some western and southern India regions suggests a potentially more favourable climate, which would be good news for agriculture and water availability in the region. However, increased dryness over the existing humid region indicates a drier future climate that will call for different agricultural and water management strategies. To tackle

the issue of desertification, the following recommendations based on "Hariyali Guidelines" (https://megsoil.gov.in/docs/HARAYALI_Guidelines.pdf accessed on August 2023) by the Department of Land Resources Ministry of Rural Development Government of India may be helpful:

- Efficient collection of precipitation for irrigation and potable water, as well as other water-intensive activities, to create a sustainable source of water and income for rural communities
- Improving weather forecasts and educating farmers and other stakeholders on effectively utilising the data to determine irrigation or crop plantation requirements to minimize water waste and increase output.
- Advancing the use of simple, low-cost, and accessible technological solutions and institutional arrangements that employ and build upon local technical expertise and readily available resources to manage water resources and related works more efficiently.

The results of this study may help identify the places that may require the aforementioned recommendations and can also help prepare guidelines for improved water distribution management in the event of future climate change. With a better understanding of the aridity trend, agricultural and water resource management can be enhanced in a way that is both sustainable and productive.

Supplementary Information The online version contains supplementary material available at https://doi.org/10.1007/s00704-023-04686-9.

Acknowledgements The authors gratefully acknowledge the partial support given by the Earth System Science Organization, Ministry of Earth Sciences, Government of India to conduct this research.

Author contribution Rajib Maity conceptualized the central idea and methodological outline. Material preparation, data curation and formal analysis were performed by Rohit Prasad Shaw and Subhra Sekhar Maity. Rajib Maity performed the investigation and review of the results. The first draft of the manuscript was written by Subhra Sekhar Maity and Rohit Prasad Shaw and it was edited by Rajib Maity. All authors commented on the previous versions of the manuscript and approved the final version of the manuscript. The work was done under the supervision of Rajib Maity.

Funding This work was partially supported by the sponsored projects supported by Ministry of Earth Sciences (MoES), Government of India through a sponsored project.

Data availability Monthly precipitation and PET data are obtained from the Climatic Research Unit (CRU) dataset (https://crudata.uea.ac.uk/cru/data/hrg/ accessed in October 2022). Digital elevation model (DEM) is obtained from Shuttle Radar Topography Mission (SRTM) (https://www.earthdata.nasa.gov/ accessed on August 2023). Soil texture data is obtained from Regridded Harmonized World Soil Database v1.2 (https://daac.ornl.gov/cgi-bin/dsviewer.pl?ds_id=1247 accessed on August 2023) (Wieder 2014) and soil depth data is obtained from the National Remote Sensing Centre (NRCS) archive of Bhuvan (https://bhuvan-app3.nrsc.gov.in/data/download/index.php accessed on August 2023).

Code availability The codes required for the analysis are written in MATLAB R2021a. The codes may be available on request from the authors.

Declarations

Competing interests The authors declare no competing interests.

References

Agnew C, Anderson E (1992) Water resources in the arid realm. Routledge, London

Ahmad F, Uddin MM, Goparaju L (2019) Agroforestry suitability mapping of India: geospatial approach based on FAO guidelines. Agrofor Syst 93:1319–1336. https://doi.org/10.1007/s10457-018-0233-7

Ahmed K, Shahid S, Chung ES et al (2020) Divergence of potential evapotranspiration trends over Pakistan during 1967–2016. Theor Appl Climatol 141:215–227. https://doi.org/10.1007/s00704-020-03195-3

Asadi Zarch MA, Sivakumar B, Sharma A (2015) Assessment of global aridity change. J Hydrol 520:300–313. https://doi.org/10.1016/j.jhydrol.2014.11.033

Barrow CJ (1992) World atlas of desertification (United nations environment programme), edited by N. Middleton and D. S. G. Thomas. Edward Arnold, London, 1992. isbn 0 3403 2, £89.50 (hardback), ix + 69 pp. L Degrad Dev 3:249–249. https://doi.org/10.1002/ldr.3400030407

Bonfils CJW, Santer BD, Fyfe JC et al (2020) Human influence on joint changes in temperature, rainfall and continental aridity. Nat Clim Chang 10:726–731. https://doi.org/10.1038/s41558-020-0821-1

Chattopadhyay N, Hulme M (1997) Evaporation and potential evapotranspiration in India under conditions of recent and future climate change. Agric for Meteorol 87:55–73. https://doi.org/10.1016/S0168-1923(97)00006-3

Choudhary A, Mahato S, Roy PS et al (2023) Analyzing the long-term variability and trend of aridity in India using non-parametric approach. Stoch Environ Res Risk Assess 4. https://doi.org/10.1007/s00477-023-02483-4

Conover WJ (2006) Practical nonparametric statistics, 3rd edn. John Willey and Sons Inc

Dangar S, Mishra V (2021) Natural and anthropogenic drivers of the lost groundwater from the Ganga River basin. Environ Res Lett 16. https://doi.org/10.1088/1748-9326/ac2ceb

Dash S, Maity R (2021) Revealing alarming changes in spatial coverage of joint hot and wet extremes across India. Sci Rep 11:1–15. https://doi.org/10.1038/s41598-021-97601-z

De Martonne E (1926) Aréisme et Indice d'Aridité. Comptes Rendus Académie des Sciences 181:1395–1398 OCLC: 492677865

D'Odorico P, Bhattachan A, Davis KF et al (2013) Global desertification: drivers and feedbacks. Adv Water Resour 51:326–344. https://doi.org/10.1016/j.advwatres.2012.01.013

Dutta R, Maity R (2022) Value addition in coupled model intercomparison project phase 6 over phase 5: global perspectives of precipitation, temperature and soil moisture fields. Acta Geophys 70:1401–1415. https://doi.org/10.1007/s11600-022-00793-9

El-Beltagy A, Madkour M (2012) Impact of climate change on arid lands agriculture. Agric Food Secur 1:1–12. https://doi.org/10.1186/2048-7010-1-3

Erinç S (1965) An attempt on precipitation efficiency and a new index; Istanbul University Institute release. Baha Press, Istanbul

Feng S, Fu Q (2013) Expansion of global drylands under a warming climate. Atmos Chem Phys 13:10081–10094. https://doi.org/10.5194/acp-13-10081-2013

Gao P, Mu XM, Wang F, Li R (2011) Changes in streamflow and sediment discharge and the response to human activities in the middle reaches of the Yellow River. Hydrol Earth Syst Sci 15:1–10. https://doi.org/10.5194/hess-15-1-2011

Goparaju L, Ahmad F (2019) Analysis of seasonal precipitation, potential evapotranspiration, aridity, future precipitation anomaly and major crops at district level of India. KN - J Cartogr Geogr Inf 69:143–154. https://doi.org/10.1007/s42489-019-00020-4

Goroshi S, Pradhan R, Singh RP et al (2017) Trend analysis of evapotranspiration over India: observed from long-term satellite measurements. J Earth Syst Sci 126:1–21. https://doi.org/10.1007/s12040-017-0891-2

Guhathakurta P, Rajeevan M (2008) Trends in the rainfall pattern over India. Int J Climatol 28:1453–1469. https://doi.org/10.1002/joc.1640

Hamed KH, Ramachandra Rao A (1998) A modified Mann-Kendall trend test for autocorrelated data. J Hydrol 204:182–196. https://doi.org/10.1016/S0022-1694(97)00125-X

Harris I, Osborn TJ, Jones P, Lister D (2020) Version 4 of the CRU TS monthly high-resolution gridded multivariate climate dataset. Sci Data 7:1–18. https://doi.org/10.1038/s41597-020-0453-3

Hartmann DL (1994) In: Hartmann DL (ed) Global physical climatology. Academic Press, San Diego

Huang J, Ji M, Xie Y et al (2016) Global semi-arid climate change over last 60 years. Clim Dyn 46:1131–1150. https://doi.org/10.1007/s00382-015-2636-8

Huo Z, Dai X, Feng S et al (2013) Effect of climate change on reference evapotranspiration and aridity index in arid region of China. J Hydrol 492:24–34. https://doi.org/10.1016/j.jhydrol.2013.04.011

IPCC (2007) Climate change 2007: Impacts, adaptation and vulnerability. In: Parry ML, Canziani OF, Palutikof JP, van der Linden PJ, Hanson CE (eds) Contribution of working group II to the fourth assessment report of the intergovernmental panel on climate change. Cambridge University Press, Cambridge, p 976

Kalyan S, Sharma D, Sharma A (2021) Spatio-temporal variation in desert vulnerability using desertification index over the Banas River Basin in Rajasthan, India. Arab J Geosci 14. https://doi.org/10.1007/s12517-020-06417-0

Kosmas C, Kirkby M, Geeson N (1999) Manual on: Key indicators of desertification and mapping environmentally sensitive areas to desertification. European Commission. Energy, Environment and Sustainable Development, EUR, 18882, p 87

Koutroulis AG (2019) Dryland changes under different levels of global warming. Sci Total Environ 655:482–511. https://doi.org/10.1016/j.scitotenv.2018.11.215

Lakshmi DD, Satyanarayana ANV, Chakraborty A (2019) Assessment of heavy precipitation events associated with floods due to strong moisture transport during summer monsoon over India. J Atmos Solar-Terrestrial Phys 189:123–140. https://doi.org/10.1016/j.jastp.2019.04.013

Latimer PH (1948) Natural evaporation from open water, bare soil and grass. Proc R Soc London Ser A Math Phys Sci 193:120–145. https://doi.org/10.1098/rspa.1948.0037

Lian X, Piao S, Chen A et al (2021) Multifaceted characteristics of dryland aridity changes in a warming world. Nat Rev Earth Environ 2:232–250. https://doi.org/10.1038/s43017-021-00144-0

Lickley M, Solomon S (2018) Drivers, timing and some impacts of global aridity change. Environ Res Lett 13:104010. https://doi.org/10.1088/1748-9326/aae013

Maity SS, Maity R (2022) Changing pattern of intensity–duration–frequency relationship of precipitation due to climate change. Water Resour Manag 36:5371–5399. https://doi.org/10.1007/s11269-022-03313-y

Mirzabaev A, Wu J, Evans J, García-Oliva F, Hussein IAG, Iqbal MH, Kimutai J, Knowles T, Meza F, Nedjraoui D, Tena F, Türkeş M, Vázquez RJ, Weltz M, 2019: Desertification. In: Climate Change and Land: an IPCC, special report on climate change, desertification, land degradation, sustainable land management food security et al (2022) Desertification. In: Climate Change and Land. Cambridge University Press, pp 249–344

Mondal A, Khare D, Kundu S (2015) Spatial and temporal analysis of rainfall and temperature trend of India. Theor Appl Climatol 122:143–158. https://doi.org/10.1007/s00704-014-1283-z

Monteith JL (1965) Evaporation and environment. Symp Soc Exp Biol 19:205–234

Mukherjee A, Saha D, Harvey CF et al (2015) Groundwater systems of the Indian Sub-Continent. J Hydrol Reg Stud 4:1–14. https://doi.org/10.1016/j.ejrh.2015.03.005

Oguntunde PG, Friesen J, van de Giesen N, Savenije HHG (2006) Hydroclimatology of the Volta River Basin in West Africa: trends and variability from 1901 to 2002. Phys Chem Earth, Parts a/b/c 31:1180–1188. https://doi.org/10.1016/j.pce.2006.02.062

Penman HL (1948) Natural evaporation from open water, bare soil and grass. Proc R. Soc. Lond A193120–145. https://doi.org/10.1098/rspa.1948.0037

Perović V, Kadović R, Đurđević V et al (2021) Major drivers of land degradation risk in Western Serbia: current trends and future scenarios. Ecol Indic 123. https://doi.org/10.1016/j.ecolind.2021.107377

Pettitt AN (1979) A Non-Parametric Approach to the Change-Point Problem Published by : Wiley for the Royal Statistical Society A Non-parametric Approach to the Change-point Problem. J R Stat Soc Ser C (applied Stat 28:126–135

Pradhan RK, Sharma D, Panda SK et al (2019) Changes of precipitation regime and its indices over Rajasthan state of India: impact of climate change scenarios experiments. Clim Dyn 52:3405–3420. https://doi.org/10.1007/s00382-018-4334-9

Ramarao MVS, Sanjay J, Krishnan R et al (2019) On observed aridity changes over the semiarid regions of India in a warming climate. Theor Appl Climatol 136:693–702. https://doi.org/10.1007/s00704-018-2513-6

Reid PC, Hari RE, Beaugrand G et al (2016) Global impacts of the 1980s regime shift. Glob Chang Biol 22:682–703. https://doi.org/10.1111/gcb.13106

Sahu N, Reddy GPO, Dash B et al (2021) Assessment on spatial extent of arid and semi-arid climatic zones of India using GIS. J Agrometeorol 23:189–193

Salam R, Islam ARMT, Pham QB et al (2020) The optimal alternative for quantifying reference evapotranspiration in climatic subregions of Bangladesh. Sci Rep 10:1–21. https://doi.org/10.1038/s41598-020-77183-y

Scheff J, Frierson DMW (2015) Terrestrial aridity and its response to greenhouse warming across CMIP5 climate models. J Clim 28:5583–5600. https://doi.org/10.1175/JCLI-D-14-00480.1

Schlaepfer DR, Bradford JB, Lauenroth WK et al (2017) Climate change reduces extent of temperate drylands and intensifies drought in deep soils. Nat Commun 8. https://doi.org/10.1038/ncomms14196

Schlef KE, Kunkel KE, Brown C et al (2023) Incorporating non-stationarity from climate change into rainfall frequency and intensity-duration-frequency (IDF) curves. J Hydrol 616. https://doi.org/10.1016/j.jhydrol.2022.128757

Sen PK (1968) Estimates of the Regression coefficient based on Kendall's Tau. J Am Stat Assoc 63:1379–1389. https://doi.org/10.1080/01621459.1968.10480934

Şen Z, Şişman E, Dabanli I (2019) Innovative Polygon Trend Analysis (IPTA) and applications. J Hydrol 575:202–210. https://doi.org/10.1016/j.jhydrol.2019.05.028

Shen L, Zhang Y, Ullah S et al (2021) Changes in snow depth under elevation-dependent warming over the Tibetan Plateau. Atmos Sci Lett 22:1–12. https://doi.org/10.1002/asl.1041

Shukla R, Chakraborty A, Joshi PK (2017) Vulnerability of agro-ecological zones in India under the earth system climate model scenarios. Mitig Adapt Strateg Glob Chang 22:399–425. https://doi.org/10.1007/s11027-015-9677-5

Shukla BP, Varma AK, Bahuguna IM (2023) Manifestation of spatially varying demarcations in Indian rainfall trends through change-point analysis (1901–2020). Environ Monit Assess 195:1–11. https://doi.org/10.1007/s10661-023-11447-8

Siswanto SY, Sule MIS (2019) The impact of slope steepness and land use type on soil properties in Cirandu Sub-Sub Catchment, Citarum Watershed. IOP Conf Ser Earth Environ Sci 393. https://doi.org/10.1088/1755-1315/393/1/012059

Soorya Gayathri M, Adarsh S, Shehinamol K et al (2023) Evaluation of change points and persistence of extreme climatic indices across India. Nat Hazards 116:2747–2759. https://doi.org/10.1007/s11069-022-05787-w

Squires VR, Gaur MK (eds) (2020) Food security and land use change under conditions of climatic variability: a multidimensional perspective. Springer Nature. https://doi.org/10.1007/978-3-030-36762-6

Sun Q, Miao C, Duan Q et al (2018) A Review of global precipitation data sets: data sources, estimation, and intercomparisons. Rev Geophys 56:79–107. https://doi.org/10.1002/2017RG000574

Thornthwaite CW (1948) An approach toward a rational classification of climate. Geogr Rev 38:55. https://doi.org/10.2307/210739

Thornthwaite CW, Mather JR (1955) The Water Balance Publ Climatol 8:5–86

Ullah S, You Q, Ali A et al (2019) Observed changes in maximum and minimum temperatures over China- Pakistan economic corridor during 1980–2016. Atmos Res 216:37–51. https://doi.org/10.1016/j.atmosres.2018.09.020

United Nations Educational, Scientific and Cultural Organization (1979) Map of the world distribution of arid regions. In: MAB technical notes no. 7

Wang W (2006) Stochasticity, nonlinearity and forecasting of streamflow processes. Ios Press

Wieder WR, Boehnert J, Bonan GB, Langseth M (2014) Regridded Harmonized World Soil Database v1.2. Data set. Available online [http://daac.ornl.gov] from Oak Ridge National Laboratory Distributed Active Archive Center, Oak Ridge. https://doi.org/10.3334/ORNLDAAC/1247

Xu D, You X, Xia C (2019) Assessing the spatial-temporal pattern and evolution of areas sensitive to land desertification in North China. Ecol Indic 97:150–158. https://doi.org/10.1016/j.ecolind.2018.10.005

Xue J, Gui D, Lei J et al (2019) Oasification: an unable evasive process in fighting against desertification for the sustainable development of arid and semiarid regions of China. CATENA 179:197–209. https://doi.org/10.1016/j.catena.2019.03.029

Yang H, Yang D (2012) Climatic factors influencing changing pan evaporation across China from 1961 to 2001. J Hydrol 414–415:184–193. https://doi.org/10.1016/j.jhydrol.2011.10.043

Zhang Q, Xu CY, Zhang Z (2009) Observed changes of drought/wetness episodes in the Pearl River basin, China, using the standardized precipitation index and aridity index. Theor Appl Climatol 98:89–99. https://doi.org/10.1007/s00704-008-0095-4

Zhu H, Du M, Yin X (2023) Oasification in arid and semi-arid regions of China: new changes and re-examination. Sustainability 15:3335. https://doi.org/10.3390/su15043335

Zotarelli L, Dukes MD, Romero CC, Migliaccio KW, Morgan KT (2018) Step by step calculation of the Penman-Monteith evapotranspiration (FAO-56 method)1. University of Florida / IFAS Extension https://www.agraria.unirc.it/documentazione/materiale_didattico/1462_2016_412_24509.pdf